Ion Dynamics in Cationic Lipid Bilayer Systems in Saline Solutions

ARTICLE *in* THE JOURNAL OF PHYSICAL CHEMISTRY B · JULY 2009

Impact Factor: 3.3 · DOI: 10.1021/jp810233q · Source: PubMed

4 AUTHORS, INCLUDING:

Markus S. Miettinen
Freie Universität Berlin
19 PUBLICATIONS **306** CITATIONS
SEE PROFILE

Ilpo Vattulainen
Tampere University of Technology
283 PUBLICATIONS **7,877** CITATIONS
SEE PROFILE

Mikko Karttunen
Technische Universiteit Eindhoven
234 PUBLICATIONS **6,265** CITATIONS
SEE PROFILE

Ion Dynamics in Cationic Lipid Bilayer Systems in Saline Solutions

Markus S. Miettinen,[†] Andrey A. Gurtovenko,[‡] Ilpo Vattulainen,[§,||] and Mikko Karttunen*[,⊥]

Department of Applied Physics, Helsinki University of Technology, Finland, Institute of Macromolecular Compounds, Russian Academy of Sciences, Bolshoi Prospect 31, V.O., St. Petersburg, 199004 Russia, Department of Physics, Tampere University of Technology, Finland, MEMPHYS-Center for Biomembrane Physics, University of Southern Denmark, Denmark, and Department of Applied Mathematics, The University of Western Ontario, London, Ontario, Canada

Received: November 21, 2008; Revised Manuscript Received: April 1, 2009

Positively charged lipid bilayer systems are a promising class of nonviral vectors for safe and efficient gene and drug delivery. Detailed understanding of these systems is therefore not only of fundamental but also of practical biomedical interest. Here, we study bilayers comprising a binary mixture of cationic dimyristoyltrimethylammoniumpropane (DMTAP) and zwitterionic (neutral) dimyristoylphosphatidylcholine (DMPC) lipids. Using atomistic molecular dynamics simulations, we address the effects of bilayer composition (cationic to zwitterionic lipid fraction) and of NaCl electrolyte concentration on the dynamical properties of these cationic lipid bilayer systems. We find that, despite the fact that DMPCs form complexes via Na^+ ions that bind to the lipid carbonyl oxygens, NaCl concentration has a rather minute effect on lipid diffusion. We also find the dynamics of Cl^- and Na^+ ions at the water−membrane interface to differ qualitatively. Cl^- ions have well-defined characteristic residence times of nanosecond scale. In contrast, the binding of Na^+ ions to the carbonyl region appears to lack a characteristic time scale, as the residence time distributions displayed power-law features. As to lateral dynamics, the diffusion of Na^+ ions within the water−membrane interface consists of two qualitatively different modes of motion: very slow diffusion when ions are bound to DMPC, punctuated by fast rapid jumps when detached from the lipids. Overall, the prolonged dynamics of the Na^+ ions are concluded to be interesting for the physics of the whole membrane, especially considering its interaction dynamics with charged macromolecular surfaces.

Introduction

Lipid bilayers are one the most fundamental structures in biology, and synthetic bilayer systems have been widely used in numerous technological and medical applications.[1] Liposomes, for example, are multipotent delivery vehicles, capable of transporting genetic material, proteins, or drug molecules into cells.[2] As both cell membranes and DNA have net negative charges, they prefer association with liposomes that carry a net positive charge.[3] *In vivo*, these structures are immersed in an aqueous solution with a considerable ionic strength; the effect of ions on a membrane depends on its structure and charge distribution.[4]

The average ion distribution in the vicinity of a charged surface is often described using the Poisson−Boltzmann theory,[5,6] a mean-field approximation treating ions implicitly as an ion cloud. The theory neglects fluctuations and correlations, the finite size of ions, and the discreteness of solvent, and therefore has obvious restrictions; pronounced deviations from its predictions emerge at the limit of high ion concentrations,[7−9] as well as in the presence of large surface charge densities or multivalent ions.[10−14] We note that there are a number of theories that go beyond the Poisson−Boltzmann approximation.[15−20]

As for a cationic lipid bilayer in water, the Poisson−Boltzmann treatment of a planar surface with a constant surface charge density, $\sigma > 0$, can be used to gain insight into the distributions of surrounding monovalent ions. In the simplest salt-free case, when only monovalent counterions are present, the ion number density at distance z from the charged plane has the form $n_-(z) = 1/(2\pi \ell_B(z + b)^2)$. The characteristic length scale $b = e/(2\pi\sigma\ell_B)$, called the *Gouy−Chapman length*, is the distance at which the electrostatic energy between an ion and the surface becomes equal to the thermal energy k_BT; its value is typically a few angstroms for lipid bilayers. The Gouy−Chapman length is also a measure of the counterion cloud thickness, i.e., the distance within which half of the counterions reside. As seen, the Gouy−Chapman length is defined by the *Bjerrum length*, $\ell_B = e^2/(4\pi\varepsilon_0\varepsilon_r k_B T)$, where e is the elementary charge, k_B is the Boltzmann constant, T is the temperature, ε_0 is the vacuum permittivity, and ε_r is the dielectric constant. The physical meaning of the Bjerrum length is the distance at which the electrostatic energy between two unit charges and the thermal energy become equal. The Bjerrum length changes considerably at the water−membrane interface. In bulk water at 323 K, ε_r is around 70, so that $\ell_B = 0.74$ nm. In contrast, inside the hydrophobic core of the membrane, the value of ε_r is much lower (∼2) and the Bjerrum length is profoundly larger ($\ell_B \sim 26$ nm).

The situation becomes more involved when salt ions are also present in the system. For the case of monovalent ions, the ion number density profiles read $n_\pm(z) = n_s((1 \mp \gamma e^{-z/\lambda_D})/(1 \pm \gamma e^{-z/\lambda_D}))^2$, with $\gamma = -b/\lambda_D + ((b/\lambda_D)^2 + 1)^{1/2}$. Here, n_s is the average number density of the electrolyte and $\lambda_D = 1/(8\pi \ell_B n_s)^{1/2}$ is the *Debye−Hückel screening length*. Beyond this characteristic distance, the electrostatic interaction of a given

* To whom correspondence should be addressed. E-mail: mkarttu@uwo.ca.
† Helsinki University of Technology.
‡ Russian Academy of Sciences.
§ Tampere University of Technology.
|| University of Southern Denmark.
⊥ The University of Western Ontario.

10.1021/jp810233q CCC: $40.75
Published on Web 06/17/2009

ion pair is screened strongly by other ions in the system. The Debye−Hückel screening length decreases when the concentration of ions in solution goes up. For instance, at 323 K, one has $\lambda_D \sim 0.95$ nm in an aqueous solution with 0.1 M monovalent salt, whereas λ_D decreases to ~0.30 nm when the salt concentration becomes 1.0 M.

The above simple model of a diffusive double layer is not, strictly speaking, applicable to lipid bilayers, since a bilayer cannot be treated as an inert flat plane. Instead, ions can interact with the bilayer and modify its structural, interfacial, and electrostatic properties. Experiments have shown that anionic[4,22−25] and cationic[26,27] membranes interact readily with their counterions (especially divalent ones), whereas the interactions of zwitterionic lipid bilayers with salt ions appear rather sensitive to the size and valency of ions.[28−41]

As for molecular-level computational studies, the increase in computing power in the past few years has made it possible to extend computer simulations beyond the relatively long relaxation times of tens to hundreds of nanoseconds required for equilibration of ions in lipid/water systems. Although most computational studies by far have focused on the effects of salt ions on zwitterionic (neutral) lipid bilayers,[33,42−53] there is also an increasing number of studies on anionic[54−59] and cationic[60,61] lipid bilayers. Most simulations have addressed the effect of ions on the structural and electrostatic properties of lipid membranes. In particular, it has been demonstrated that cations (e.g., Na^+ ions) are able to penetrate rather deep in the lipid headgroup region. This effect has been observed in zwitterionic,[33,42,46,50−53] anionic,[55,56,58] and slightly cationic[61] lipid bilayers. The findings agree with experimental data.[33,35,36,40,41]

Considerably less attention has been paid to the dynamical properties of lipid bilayers under the influence of salt and to the dynamics of ions in lipid/water systems. Böckmann et al. studied the effects of salt on lipid diffusion and estimated the typical times required for different ions to bind on a membrane.[33,44] As far as the dynamics of ions in lipid systems is concerned, to the best of our knowledge, the recent computational studies by Sachs et al.,[45] Patra and Karttunen,[62] and Gurtovenko and Vattulainen[47,50] are the only ones. The number of experimental studies is also limited.[40,63] Given the importance of ion dynamics in the vicinity of membranes in many biological phenomena, starting from action potentials in nerve cells[64,65] and ranging from cell energetics[66] to ion-mediated signaling between active membrane proteins,[67−69] the lack of computational studies on ion dynamics is rather surprising.

To understand the dynamics of ions in a lipid/water system, we have studied charged (cationic) lipid bilayers in saline solutions. We have employed atomic scale molecular dynamics (MD) simulations and investigated bilayers containing zwitterionic dimyristoylphosphatidylcholine (DMPC) and cationic dimyristoyltrimethylammoniumpropane (DMTAP) in aqueous solutions with NaCl salt. The DMTAP mole fraction and NaCl concentration were systematically varied; see Table 1.

In contrast to our previously published study,[61] the main focus of this work is on the dynamic behavior of co- (Na^+) and counter- (Cl^-) ions within the charged lipid−water interface and in bulk saline solution. To perform an accurate analysis of ion dynamics, the MD simulations were extended up to 242 ns (Table 1). Special attention was given to Na^+ ions, which are known to bind to the carbonyl oxygens of the zwitterionic DMPC lipids when the DMTAP fraction is small.[61] The residence times of Na^+ ions were analyzed with a particular focus on the slow fluctuations in the number of ions bound to the membrane. Furthermore, the lateral movement of Na^+ ions within the bilayer surface was studied. To complement the overall picture, we also analyzed the lateral diffusion of lipid molecules.

TABLE 1: Summary of MD Simulations of DMPC/DMTAP Lipid Bilayers[a]

χ_{TAP} (%)	[NaCl] (M)	#Na^+	t_{eq} (ns)	t_m (ns)	t_{tot} (ns)
75	0.0	0	30	110	140
	0.1	10	11	110	121
	0.5	49	11	110	121
	1.0	96	11	110	121
50	0.0	0	40	150	190
	0.1	10	20	190	210
	0.5	48	20	180	200
	1.0	94	20	170	190
6	0.0	0	31	110	141
	0.1	9	32	110	142
	0.5	46	30	130	160
	1.0	89	12	230	242
0	0.0	0	20	110	130
					2.1 μs

[a] χ_{TAP} is the molar DMTAP percentage, [NaCl] is the concentration of NaCl salt, #Na^+ is the number of Na^+ ions, t_{eq} is the equilibration time,[61] t_m is the time used for measurements, and t_{tot} is the total simulation time for each system. The setups at each χ_{TAP} stemmed from corresponding final configurations of our DMPC/DMTAP study without salt,[60,71] but expecting salt ions to bind with water molecules, we increased the number of H_2O molecules by 50%. After pre-equilibration of 20 ns, we made four copies of each mixed bilayer system and, to implement salt, replaced proper amounts of random water pairs by Na^+−Cl^- pairs.

The rest of the paper is organized as follows: The next two sections describe the simulation details and analysis methods. They are followed by two separate sections, the first of which presents the results and the latter provides a discussion and comparison with previous research. We finish with a summary and conclusions.

Simulation Details and Setup

We performed atomic scale molecular dynamics simulations of one neutral and 12 cationic lipid bilayers in aqueous solutions with and without NaCl salt (Table 1). Each bilayer comprised a mixture of cationic dimyristoyltrimethylammoniumpropane (DMTAP) and zwitterionic dimyristoylphosphatidylcholine (DMPC) lipids; see Figure 1. Lipid contents of the two leaflets were identical, and in addition to the 128 lipids, each system contained as many Cl^- counterions as DMTAPs: 8 (at $\chi_{TAP} =$ 6%), 64 (50%), or 96 (75%). To guarantee full lipid hydration with the addition of NaCl (Table 1), each system had over 5000 water molecules. All systems were charge neutral.

Lipids were treated within the united-atom description; DMTAP has 39 and DMPC 46 interaction sites. For DMPC, we used the force-field of Berger et al.,[70] and for DMTAP, the parameters developed by Gurtovenko et al.[60] Both force-fields are available online.[71] For Na^+ and Cl^- ions, we employed the GROMACS force-field,[72−74] and for water, the SPC (simple point charge) model.[75]

The Lennard-Jones interactions were truncated at 1 nm. For the electrostatic interactions, we used the particle-mesh Ewald method[76,77] (with fourth-order interpolation, real space cutoff at 1 nm, the relative error in the direct and reciprocal space 10^{-5}, and fast Fourier transform parameters optimized for the box size), which has been shown to perform well in membrane simulations.[78−80] In lipids, all covalent bonds were constrained to their equilibrium lengths by LINCS (LINear Constraint Solver)[81] and in water molecules by SETTLE.[82]

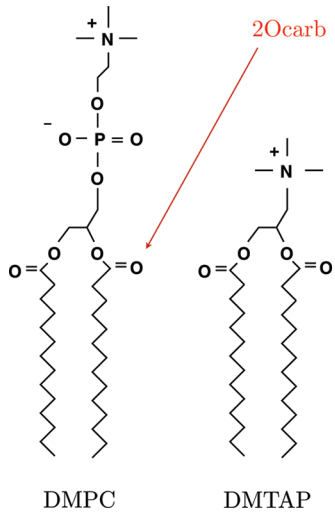

Figure 1. Structures of DMPC and DMTAP lipid molecules. The complexation of DMPCs takes place through Na^+ binding to the carbonyl oxygen of the *sn-2* chain, "2Ocarb".[61]

The main transition temperature, T_m, at atmospheric pressure is 296 K for a pure DMPC bilayer,[83] while it is around 311 K for a pure DMTAP bilayer.[84] For DMPC/DMTAP mixtures, T_m depends on the molar fraction of DMTAP, χ_{TAP}; experiments at 3 bar[85] have shown that $T_m(\chi_{TAP})$ is downward concave and has a global maximum of 310 K at around $\chi_{TAP} \sim 45$ mol %. Therefore, all of the simulations were performed at 323 K to simulate the fluid phase.

Temperature and pressure (set to 1 bar) were controlled by the weak coupling method.[86] Heat bath coupling of lipids was separate from the rest of the system, and both subsystems had coupling time constants of 0.1 ps. Pressure coupling (time constants set to 1.0 ps) was applied semi-isotropically, i.e., the extension of the simulation box in the bilayer normal direction (z) and its cross-sectional area in the bilayer plane (xy) were able to vary independently. Periodic boundary conditions were applied in all three directions. The time step was set to 2 fs, and particle positions saved every 10 ps.

We studied three different mixtures of DMPC and DMTAP lipids with the molar fraction of DMTAP (χ_{TAP}) being equal to 6, 50, and 75 mol %. Each of these bilayers was simulated 4 times: without salt and with 0.1, 0.5, and 1.0 M of NaCl salt; see Table 1. Furthermore, we performed an additional simulation of a pure DMPC bilayer in a salt-free aqueous solution.

Each simulated system consisted of over 21 000 atoms. The total simulated time was 2.1 μs, the longest individual simulation run amounting to 242 ns; see Table 1. All simulations were performed using the GROMACS suite.[72−74]

Data Analysis

Lateral Diffusion of Lipids. To study the lateral dynamics of lipids, we measured the lateral (2D) self-diffusion coefficient for each lipid species α

$$D_\alpha = \lim_{t\to\infty} \frac{1}{4t}\langle r^2(t)\rangle = \lim_{t\to\infty} \frac{1}{4tN_\alpha}\sum_{i=1}^{N_\alpha}\langle r_i^2(t)\rangle \qquad (1)$$

Here, $\langle r_i^2(t)\rangle$ is the average (during t_m, see Table 1) squared lateral displacement of the i^{th} lipid (of type α) in time t. To exclude leaflet movement, we measured the displacements of lipid centers of mass, r_i, with respect to the centers of mass of their respective leaflets. N_α is the total number of lipids of type α in the system. The slope of the mean squared displacement (MSD), $\sum_{i=1}^{N_\alpha}\langle r_i^2(t)\rangle/N_\alpha$, at the limit of the longest available time scale (fitting started from 10 and ended to 25 ns), provided D_α. The errors were evaluated from the variation of $\langle r_i^2(t)\rangle$ of individual lipid molecules.

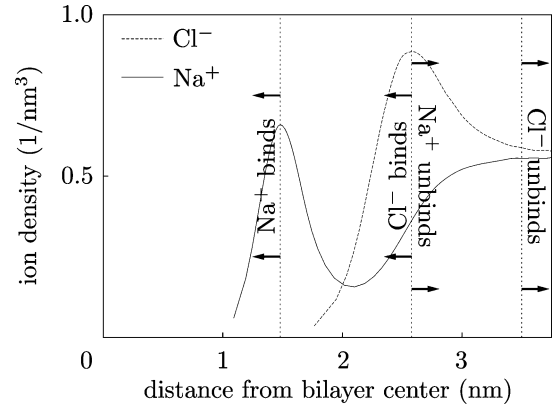

Figure 2. Visualization of definitions for ion binding and unbinding in residence time measurements. Here, $\chi_{TAP} = 6\%$ and [NaCl] = 1.0 mol, other systems analogously; see Table 2.

Ion Diffusion in Bulk Water. To characterize ion dynamics along the direction of the bilayer normal, the z-coordinates of each ion were recorded at 10 ps intervals over 50 ns. The origin was fixed to the center of mass of the bilayer to eliminate the effect of bilayer movement. From these data, we constructed a two-dimensional histogram, $z(t + \Delta t)$ versus $z(t)$, in order to visualize how the position of an ion at time t influences its position at time $t + \Delta t$. Bins in the histogram were 0.1 nm × 0.1 nm, and its volume was normalized to unity.

Ion Residence Times. We performed a more quantitative analysis of ion dynamics by focusing on the "basin of attraction" for each ion type. For Na^+ ions, this is the lipid carbonyl region, and for Cl^-, the water−lipid interface. To study the residence times, we used the following definitions for ion binding (see also the illustration in Figure 2). A Na^+ ion was considered to be bound to the lipid carbonyl region if it got closer to the bilayer center than the peak in the Na^+ distribution and until it moved further away than the Cl^- ion peak. Analogously, a Cl^- ion was considered to be bound from the moment it moved closer to the bilayer center than the Cl^- peak, and until it escaped into bulk water. All of the values used in these definitions are given in Table 2; if there is no peak (Table 2), then there is no residence time. We used different limits for binding and unbinding, because we wish to separate small fluctuations, or "flicker motion", in an ion's position from the actual binding/unbinding events. The results are robust to the choice of the unbinding limit, as it simply functions as a filter for small fluctuations; this was separately tested by varying the unbinding limit. In addition, the use of two limits helps to identify the true binding events, as ions are not considered bound until they penetrate deep enough. After that, they are allowed some freedom; e.g, a Na^+ ion jumping from one carbonyl oxygen to another does not count as unbinding, even if the ion would move a bit away from the bilayer center during the jump. To determine the residence time distributions, we created histograms for the durations of all binding−unbinding events during t_m (Table 1). The bin-wise errorbars of the histograms were estimated as standard errors of the mean bin height.

Salt Asymmetry. We define salt asymmetry as the difference in the number of ions bound to the two leaflets. Instantaneous coordination numbers will always differ, as binding of ions is

TABLE 2: Values for Na^+ and Cl^- Peaks and the Distances from the Bilayer Center at Which Cl^- Ions Become Unbound as Used in the Calculation of Residence Times; See Figure 2

χ_{TAP} (%)	[NaCl] (M)	Na^+ peak (nm)	Cl^- peak (nm)	Cl^- unbound (nm)
6	0.0		2.59	3.5
	0.1	1.335	2.54	3.5
	0.5	1.465	2.53	3.5
	1.0	1.480	2.58	3.5
50	0.0		2.16	4.0
	0.1	1.56	2.19	4.0
	0.5	no	2.24	4.0
	1.0	1.62	2.28	4.0
75	0.0		1.94	3.75
	0.1	no	1.96	3.75
	0.5	no	2.00	3.75
	1.0	no	2.02	3.75

dynamic, but in equilibrium, the average coordination numbers must be the same. Thus, measuring salt asymmetry provides a possible way to investigate equilibration and the time scales involved. In addition, it offers a method to study if those time scales differ between the different ion types. We counted the number of ions bound to each "basin of attraction" (Figure 2) every 10 ps. These numbers were plotted as a function of the simulation time t.

Na^+ Diffusion within the Carbonyl Region. To study the lateral diffusion of Na^+ ions residing within the carbonyl region, we measured their lateral MSDs during residence. To exclude the possible effects from leaflet movement, the measurements were done with respect to the center of mass of the leaflet. Regarding each binding−unbinding event (Figure 2) as giving an independent $\langle r_i^2(t)\rangle$, we used the same method for determining the error estimates as described for lipid diffusion above.

As Na^+ and DMPC are known[61] to complex via the carbonyl oxygen "2Ocarb", see Figure 1, we studied how complexing affects the diffusion mechanism of Na^+. We used the Na^+−2Ocarb distance (<0.28 nm) to identify complexes of one, two, three, or four DMPCs, uncomplexed Na^+, and uncomplexed DMPC. Within each of these groups, lateral MSDs were measured, regarding each existence of a complex as giving an independent $\langle r_i^2(t)\rangle$. A given complex was considered to exist as long as it comprised exactly those molecules that originally formed it. As the complex half-lives exceeded nanoseconds, the possibility of a complex breaking and reforming between consecutive saved simulation frames (10 ps) should not impact the results.

Results

Lateral Diffusion of Lipids. Typical lateral diffusion coefficients measured for lipids (for DMPC, see, e.g., Filippov et al.[87]) in biomembranes are of the order of $10^{-8}-10^{-7}$ cm^2/s, corresponding to net distances from a few angstroms to a few nanometers traversed in 100 ns.[88] Studying lipid diffusion via atomic scale molecular simulations thus requires maximal measurement times, especially since diffusion may involve complex collective motions.[21,89]

Here, three qualitative trends emerged, as displayed in Figure 3: (1) under all conditions, both lipid types behaved rather similarly, the difference between them falling within error bars; (2) increase in χ_{TAP} hastened diffusion slightly in the mixed bilayers (for pure DMPC, $D = (1.29 \pm 0.15) \times 10^{-7}$ cm^2/s); (3) NaCl did not have any noticeable effect on lipid diffusion, except for the slight slowdown it caused in $\chi_{TAP} = 6\%$ systems.

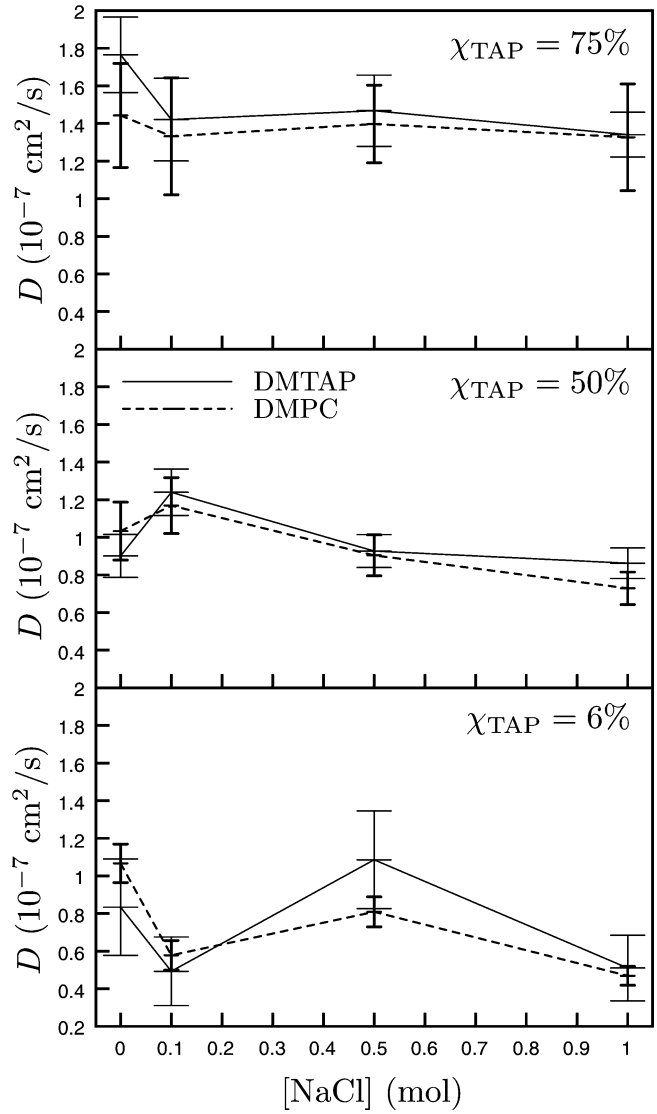

Figure 3. Lateral self-diffusion coefficients D of DMPC and DMTAP as a function of salt concentration [NaCl] for the three different DMTAP molar fractions. In these mixed bilayers, adding DMTAP accelerated lipid diffusion slightly; $D = 1.29 \pm 0.15 \times 10^{-7}$ cm^2/s for pure DMPC.

Ion Diffusion across Bulk Water. Now, we take a look at ion diffusion in water. As Figure 2 illustrates, and as also seen in our previous study,[61] the forms of Cl^- and Na^+ distributions through a DMPC/DMTAP bilayer system differ qualitatively. They reflect the average charge distribution of lipids, which, were it *a priori* known, could be used as the boundary condition for numerically estimating the ion distributions from the Poisson−Boltzmann theory (c.f. the Introduction and Böckmann et al.[33]). At all χ_{TAP}, the Cl^- ions form a compensating layer next to the positively charged wall, whereas the Na^+ distribution is qualitatively χ_{TAP} dependent. At low χ_{TAP} (6%), Na^+ binds to the negatively charged carbonyl region, but at higher χ_{TAP} (50% and especially 75%), Na^+ populates only the intermembrane water layer.[61]

These qualitatively different spatial distributions of Na^+ and Cl^- correspond to qualitatively different dynamics, as is illustrated in Figure 4 for two different DMTAP molar fractions (6 and 75%). Separation of time scales between Na^+ release from the carbonyl region ($\gg$10 ns) and ion diffusion across the intermembrane bulk water (<10 ns) is evident. The movement of Na^+ ions not bound in carbonyl regions resembles free

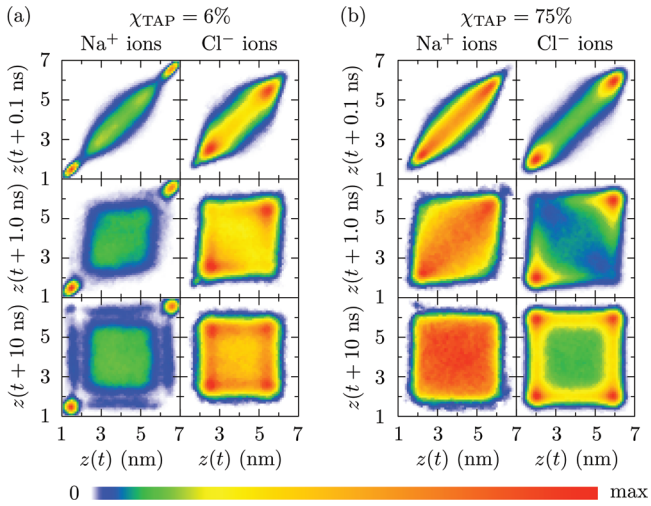

Figure 4. At $\chi_{TAP} = 6\%$, Na^+ is bound strongly to the carbonyl region. The panels describe movement of ions in the direction of the bilayer normal during three time intervals: 100 ps, 1 ns, and 10 ns. Positions are described by $z(t)$, the (smallest positive) distance from the bilayer center at time t; $z(t + \Delta t)$ is the same at time $t + \Delta t$. Blue color means that just a few ions move from $z(t)$ to $z(t + \Delta t)$ during time Δt. Red indicates the opposite. To achieve good contrast even when the distribution spreads, the colors were scaled from zero to the maximum bin value separately for each panel. The "max" values were (top to bottom and left to right) (a) 1.01, 0.73, 0.55; 0.39, 0.17, 0.12 and (b) 0.31, 0.12, 0.08; 0.57, 0.33, 0.16. Here, [NaCl] = 1.0 M and the measurement is over 50 ns.

diffusion, and they seem indifferent to the positively charged walls. This indicates the effectiveness of the Cl^- counterion layer in screening the cationic bilayer surface to appear as effectively neutral to the intermembrane bulk water. As for Cl^- ions then, the time scale separation between those ions residing in the diffuse counterion layer and the ones crossing the bulk water is less striking, although the positively charged surface is able to hold its counterions for several nanoseconds.

Figure 4 only shows the [NaCl] = 1.0 M case, but as the effects of salt concentration on Na^+ or Cl^- dynamics were weak, the other NaCl concentrations appeared qualitatively similar. Next, we describe the ion dynamics quantitatively.

Ion Residence Times. Interestingly, the residence time distributions of Na^+ (in the carbonyl region) and Cl^- (at the water−lipid interface) were strikingly dissimilar (Figure 5).

The Cl^- ion residence times, t, followed an exponential distribution, $\exp(-t/\tau)$, with characteristic decay time, τ. A fit to the linear part of the log−linear plot gave the decay time constant τ as the negative inverse of the slope of the fitted line. These characteristic times are given in Figure 6 as a function of NaCl concentration.

Contrary to Cl^-, sodium appeared to follow a power law, t^β, with no characteristic time scale. This explains the long residence times (strongly localized peaks) in Figure 4a. A fit to the linear part of the log−log plot gave the exponent β. It could only be determined for $\chi_{TAP} = 50\%$ with [NaCl] = 1.0 M ($\beta = -1.6$), and the $\chi_{TAP} = 6\%$ systems ($\beta = -0.9$ for [NaCl] = 0.1 M and −1.0 for both 0.5 and 1.0 M). In other systems, there were no, or too few, binding events despite the rather long measurements (t_m in Table 1). The error was estimated to be ±0.2 in all of the cases. At very short times ($t < 1$ ns), see Figure 5, there is a deviation from power-law behavior. From our data, we cannot conclusively define the functional form for Na^+ residence time distribution. We can, however, make the conclusion that the distribution decays very slowly.

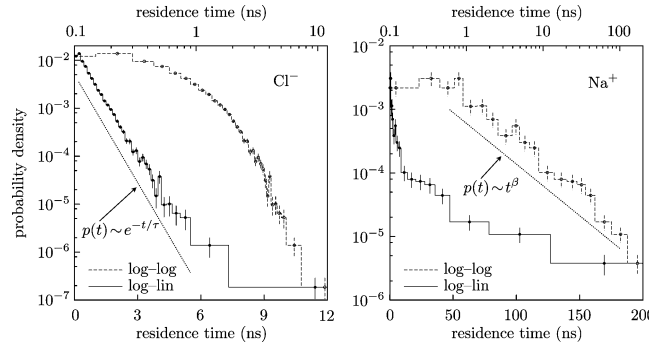

Figure 5. Residence time distributions of co- and counterions appeared qualitatively different. The left panel shows the residence time distribution of Cl^- ions in the attractive region at the water−lipid interface (see Figures 2 and 4). The right panel shows the distribution of residence times of Na^+ ions in the attractive carbonyl region (see Figures 2 and 4). In each panel, the two curves show the same data, but the dashed curve is on a log−log scale and the solid curve is on a log−lin scale to reveal the different functional forms of the distributions. Here, $\chi_{TAP} = 6\%$ and [NaCl] = 1.0 M.

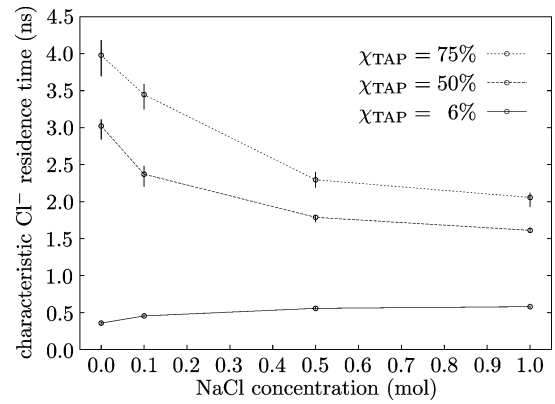

Figure 6. Surface charge enhanced and salt weakened Cl^- binding. Characteristic residence times, τ, of Cl^- ions as a function of NaCl concentration for the three different molar fractions of DMTAP.

Returning to Cl^- residence times, salt concentration and surface charge had expected (as discussed in the Introduction) effects on τ as Figure 6 shows: (1) higher bilayer surface charge σ (higher χ_{TAP}), and thus shorter Gouy−Chapman length b, leads to an attraction of counterions closer to the surface. Tighter binding of ions is reflected as longer characteristic residence times τ. (2) Higher [NaCl] means shorter Debye−Hückel screening length λ_D and thus an increase of the ratio b/λ_D, allowing the ion cloud to extend further from the bilayer surface. This looser binding is reflected as shorter residence times τ. (3) The slightly increasing trend in τ as [NaCl] increases in the case of low χ_{TAP} (6%) resulted, most likely, because with higher [NaCl] more Na^+ ions are able to bind to the DMPCs and thus increase the positive surface charge σ (see also Figure 14 in Gurtovenko et al.[61]), decrease b, and increase τ.

Salt Asymmetry. At $\chi_{TAP} = 6\%$, in concert with the long-lived binding of Na^+ ions to the carbonyl region, long-lived asymmetries in ion content between monolayers developed (Figure 7). The fluctuations in the number of bound Na^+ ions were slow, taking place in tens of nanoseconds. Although fluctuating more vigorously, the number of attracted Cl^- ions per leaflet followed that of bound Na^+.

Na^+ Diffusion within the Carbonyl Region. The average lateral motion of Na^+ ions was not considerably faster than that of lipids (Figure 8). Interestingly, however, we found Na^+ diffusion to comprise two qualitatively different modes: When

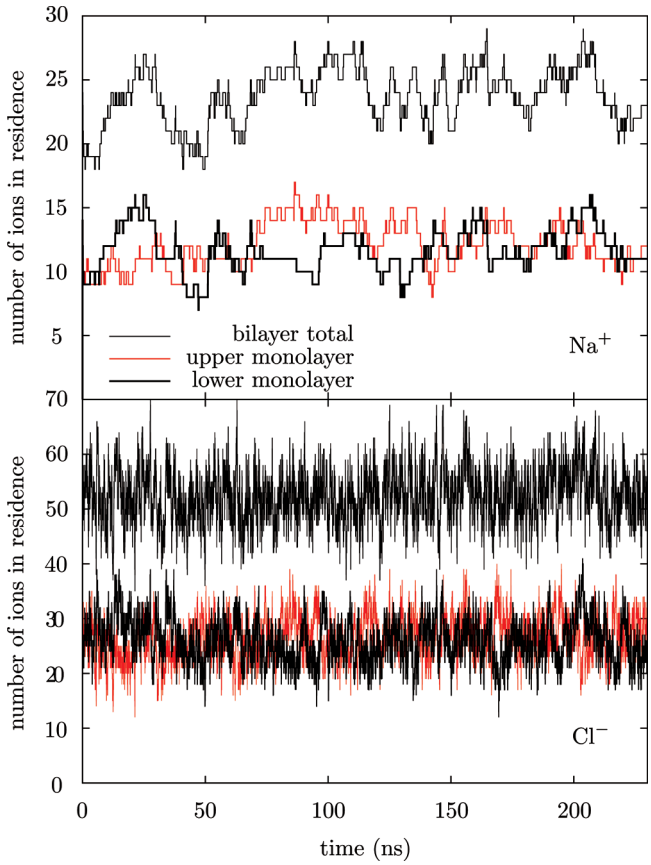

Figure 7. Long-lived asymmetries in ion content between leaflets at low χ_{TAP}. The Na^+ content of leaflets varied slowly, with changes taking place in tens of nanoseconds. This correlated with the amount of Cl^- attracted to the monolayer vicinity. The latter, however, showed much faster fluctuations and faster relaxation. Here, $\chi_{TAP} = 6\%$ and [NaCl] = 1.0 M.

complexed with DMPC, Na^+ diffuses slowly, whereas, when free of DMPCs, it moves in a rapid "hopping" fashion (Figure 9). The inset in Figure 9 also shows that the bigger the complex around a Na^+ ion, the slower the ion diffuses. This agrees with Figure 8, which shows Na^+ diffusion to be slowest at [NaCl] = 0.1 M, i.e., when the three- and four-DMPC clusters are more likely to bind Na^+ than at higher [NaCl]. Looking at the inset for DMPCs in Figure 9, it is curious to note that just binding a Na^+, i.e., not even complexing with other DMPCs via it, suffices to slow the short-time DMPC diffusion considerably.

The lifetime distributions of complexes and free Na^+ did not have forms describable with an average or a single relaxation time. The time scale difference between a free Na^+ and that bound to a complex can, however, be estimated via the half-time, i.e., the time it takes for a free ion (or an ion in a complex) to bind to a complex (or to become free) with a 50% probability. For a free Na^+ within the carbonyl region, this was about 300 ps for all three [NaCl]. For a complexed Na^+, however, this time was an order of magnitude longer: 20 ns (0.1 M), 9 ns (0.5 M), 12 ns (1.0 M).

Discussion

The dynamics of ions within a lipid bilayer system has been mostly overlooked in the literature until very recently. That is understandable, as simulations have to be very long, even with current computational resources.[33] Our simulations, spanning 2.1 μs in total, show that ion dynamics within a cationic lipid bilayer system possesses intriguing features, and may even be qualitatively different for different ion types, as demonstrated in Figure 5. Hence, let us start the discussion by focusing on the dynamics of ion binding to, and unbinding from, the membrane.

Ion Residence Times. To the best of our knowledge, we are the first to report a detailed study of residence times. The Cl^- counterions were found to have exponentially distributed residence times (Figure 5), with characteristic times in the nanosecond region (Figure 6). The Na^+ ions, in contrast, appeared to have residence time distributions with no characteristic time scale; i.e, they had a power-law-like distribution in the time scales accessible to this study and current MD simulations (Figure 5).

The exponentially distributed residence times of Cl^- ions are explained simply with a Poisson process (c.f. radioactive decay). This points to the direction that binding of a Cl^- ion to the wall (membrane) is effectively independent of other Cl^- ions. The behavior of Cl^- residence times may thus be qualitatively extrapolated from the simple electrostatic double layer model described in the Introduction.

The slowly decaying long time distribution for Na^+ ions, on the other hand, is quite intriguing, and no simple explanation is available. Comparison with experiments or other simulations is not possible, as these properties, as far as we know, have not been studied quantitatively. Sachs et al.[45] computed the residence times as a function of distance from a zwitterionic phosphatidylcholine bilayer, but their simulations spanned only 5 ns and an exponential distribution of residence times was assumed, not confirmed. They did, however, observe that the behavior of Na^+ and Cl^- ions was different, and that the time scales related to Na^+ were longer.[45] Our considerably longer simulation times enabled us to see more detail in the diffusion behavior, in particular that of Na^+ ions.

Although with only one ion species present, Patra and Karttunen[62] studied the probability $P(d,t)$ that a Cl^- ion moves a distance d in time t in cationic sphingosine bilayers and found that under certain conditions the counterion cloud exhibits two-fluid behavior. From the point of view of the current study, this indicates that the behavior of ions in the vicinity of charged membranes may indeed be more complex than expected. The above is also supported by the observations from comparisons of water dynamics in the immediate vicinity of charged and zwitterionic bilayers;[90] water dynamics, translational and rotational, are strongly influenced and slowed down by the presence of charges in a nontrivial manner. Before moving to other topics, we would like to mention that ion specific behavior has also been seen in other systems, and there are suggestions that the observed effects may be due, among other possibilites, to Hofmeister phenomena.[91]

Lateral Diffusion of Lipids. Perhaps surprisingly, in our extensive atomistic simulations, NaCl concentration had only a minute effect on the lipid lateral diffusion (Figure 3). The slight slowdown at $\chi_{TAP} = 6\%$ is, in light of Figure 9, associated with the Na^+−DMPC clustering taking place in these systems. A change of roughly similar relative magnitude was reported by Böckmann et al.[33] upon adding NaCl to a POPC bilayer. Clustering has also been observed to be of importance in anionic bilayers.[58]

The effect of DMTAP molar fraction on lipid diffusion (Figure 3) appears to be closely linked to the free volume per lipid. For salt-free systems, adding some DMTAP to a DMPC bilayer is known to decrease the area per lipid,[60] as the cationic lipids "stitch" the DMPCs together.[92] After a limiting value (χ_{TAP} = 50%[60]), however, the average free volume begins to increase,

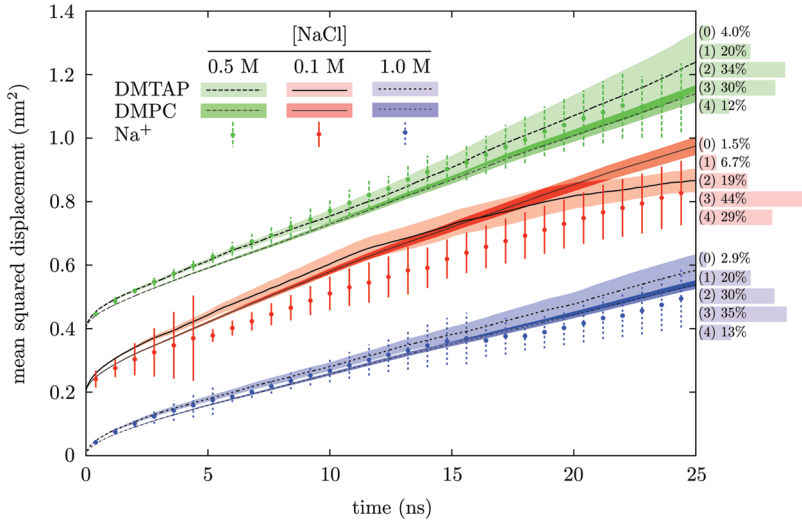

Figure 8. Lateral mean squared displacements of lipid molecules and Na^+ ions in those systems where Na^+ binds to the carbonyl region, $\chi_{TAP} = 6\%$. The colored regions of lipid MSDs, and the error bars of the Na^+ MSDs represent the standard errors of the MSD, measured as explained in the text. Note that the 0.1 M curves have been shifted by 0.2 nm^2, and 0.5 M by 0.4 nm^2, to make the plot read better. The respective histograms on the right show the percentage of time that a Na^+ ion bound to the carbonyl region spends uncomplexed (0) or in complexes of one to four lipids (1−4).

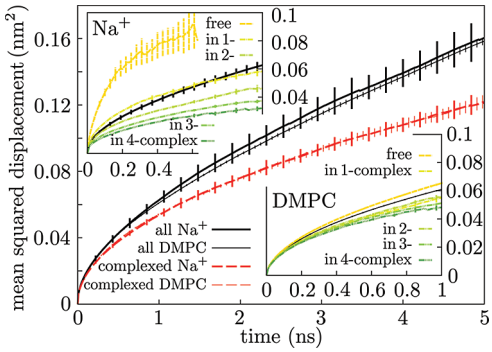

Figure 9. Hopping greatly promoted the lateral diffusion of Na^+ within the carbonyl region. The lateral mean squared displacement (MSD) of sodiums continuously complexed with DMPC (thick dashed red line) is considerably smaller than if lipid-free hops are allowed (thick continuous black). The insets for Na^+ and DMPC show their subnanosecond lateral MSDs separately for uncomplexed (free) and for each complex size (1, 2, 3, or 4 DMPCs). In order to focus solely on Na^+ hopping, we have used only that part of the carbonyl-bound Na^+ trajectories that starts from Na^+ entering the first complex and ends with Na^+ leaving the last complex. Here, [NaCl] = 1.0 M and $\chi_{TAP} = 6\%$.

as in DMTAP the headgroup is smaller than in DMPC, and as electrostatic repulsion increases the area per lipid. As one expects more free volume to lead to faster lipid diffusion, these findings agree with our results in Figure 3.

An interesting subject for further study would be to elucidate the mechanism behind the somewhat unexpected observation that just binding a Na^+ slows a DMPC considerably (inset in Figure 9). This could result from, e.g., an increase in the relaxation time of the carbonyl vector due to the extra positive charge, or an attraction of the bound Na^+ by the carbonyls of other DMPCs.

Na^+ Diffusion within the Carbonyl Region. We find that on average Na^+ ions appear to diffuse laterally no faster than the lipids (Figure 8), but interestingly, they perform two different types of motion: Slow diffusion along with the DMPCs when complexed and fast rapid hops when uncomplexed (Figure 9). Hopping occurs rapidly on a subnanosecond time scale, and is fast considering the distance covered, thus making an important contribution to the Na^+ diffusion along the membrane. We are not aware of any other studies reporting the lateral hopping motion of Na^+ ions we describe here, but the diffusional behavior and transport of protons close to and along bilayer surfaces has proven to be very rich[93] and the behavior observed for positive Na^+ ions here could be related to some degree to the behavior of protons.

Measuring the long-time lateral diffusion coefficients for Na^+ from Figure 8 gives D_{Na^+} of the same order as that for the lipids (Figure 3), i.e., $D \approx 0.7 \times 10^{-7}$ cm^2/s, which is surprisingly close to the experimental results of Rigaud et al.,[63] reporting $D_{Na^+} \approx 0.7 \times 10^{-7}$ cm^2/s at the limit of low water content, i.e., when all of their Na^+ are in principle bound to the bilayer.

Salt Asymmetry. We find that rather large and long-lived asymmetries develop between bilayer leaflets (Figure 7) because of the prolonged binding of Na^+ ions. These asymmetries are, however, not long-lived or strong enough to cause pore formation, reported for asymmetric bilayer systems.[47] They should, however, be taken into account when evaluating if a system containg ions has reached its equilibrium, as well as when estimating the simulation times required to get meaningful averages from such systems.

Ion Diffusion across Bulk Water. We find that ion diffusion across bulk water takes place in nanoseconds, except for the Na^+ ions in the low χ_{TAP} systems, in which the sodiums can associate with the carbonyl region for much longer times; see Figure 4. The key question concerning the relevance of our findings is if the strong coordination of Na^+ ions by the DMPC carbonyl oxygens at low χ_{TAP} is a real effect or a model artifact. Let us thus review here the relevant literature.

Until rather recently, Na^+ ions were thought to be rather indifferent cations with respect to phospholipids,[94,95] and ion binding in general to take place only in the headgroup region.[28,30] During the past decade, however, this view has been challenged. Indirect evidence from infrared spectroscopy,[32] fluorescence correlation spectroscopy,[33] atomic force microscopy,[35,36] small-angle X-ray diffraction,[41] spin-labeling electron paramagnetic resonance spectroscopy,[41] and calorimetric[33,41] studies suggest the possibility of Na^+ interacting with lipid carbonyl oxygens, binding lipids into complexes, and thus leading to detectable changes in area per lipid, bilayer thickness and rigidity,[41] as

well as lipid lateral diffusion,[33] main transition temperature, calorimetric peak width,[33,41] and increase of force required to puncture the bilayer in the gel phase.[35,36] In addition to this indirect evidence, direct images of possible ion or water bridges between lipids below headgroups have been provided by frequency modulation atomic force microscopy of supported phosphatidylcholine bilayers in the gel phase.[40]

These experimental results have emerged in unison with the first realistic atomistic simulations on effects of ions on lipid bilayers—made feasible only by the immense increase in computing power during the past few decades, as the equilibration times for ion binding to a bilayer are of the order of tens to hundreds of nanoseconds.[33] This simulational work at the atomistic level can be divided roughly into two categories, depending on the force-field used to describe the lipids. Using the all-atom CHARMM (Chemistry at HARvard Molecular Mechanics) parameter set 27, no complexation of Na^+ with the lipid carbonyl oxygens has been reported.[43,45,57] In contrast, using the "Berger lipids", i.e., variants of united-atom force-fields based on refs 70, 96, and 97, tight binding of Na^+ ions to the lipid carbonyl oxygens is found.[33,42,46,50−53,55,56,58,61] Due to the different nature of these two force-fields, simulations using CHARMM27 lipids need to be performed with the area of the bilayer fixed, whereas Berger lipids allow simulations in the *NpT* ensemble, such that the bilayer can adjust its area to agree with the thermodynamic parameters. Furthermore, the carbonyl region of lipid molecules is more polar in the case of the Berger force-field, so that it attracts cations considerably stronger compared to its CHARMM counterpart. Interestingly, Shinoda et al.,[49] who modified the CHARMM27 force-field replacing the ester groups with their self-developed ether groups to simulate an archaeal lipid bilayer, were able to use the *NpT* ensemble and found Na^+ binding to the ether oxygens.

Typical choices for water model and ion force-fields used with Berger lipids are the ones used in the present study. The results on Na^+ binding acquired using the Berger lipids, however, seem not to be qualitatively changed if the water model is changed[53] or if the CHARMM27 force-field is used for the ions.[50,52] The ion force-fields for Na^+ and Cl^- (Gromacs, Charmm-27/22, Amber, OPLS-AA) with different combinations of water models have been systematically tested,[98] and although there are some deviations, they are qualitatively in agreement. More serious problems, however, have been demonstrated for some K^+ force-fields.[99]

Summary and Conclusions

This is, to our knowledge, the first systematic report on ion dynamics in charged bilayer systems. In agreement with previous studies, we see differences in residence times and binding behavior between the different ion species. The most surprising and new finding here is that the residence times of Na^+ were observed to be so long that they did not appear to have a characteristic time scale within our simulational time frame of the order of hundreds of nanoseconds. The origin of the power-law-like features of Na^+ ion residence dynamics remains unclear, though.

In this paper, we note that the systems having low cationic lipid content are able to retain cationic ions in their carbonyl region for very long times, whereas systems with higher cationic lipid content lack this ability. This encourages one to speculate on the possibility of signaling via changes in cationic lipid content, leading to a rapid release of cationic ions from the bilayer. More generally, should membranes' capability of retaining positive ions have biological relevance, one is lead to speculate if this could be part of the explanation for the observed scarcity of cationic lipids in biological membranes.

Acknowledgment. This work has been supported by the National Graduate School in Materials Physics (M.S.M.), the Russian Foundation of Basic Research through Grant No. 08-03-00150 (A.A.G.), the Academy of Finland (I.V., M.K.), Emil Aaltonen Foundation (M.K.), and Magnus Ehrnrooth and Vaisala Foundations (M.S.M.) and NSERC of Canada (M.K.). We would like to thank the Finnish IT Center for Science, the HorseShoe (DCSC) supercluster computing facility at the University of Southern Denmark, and SharcNet (www.sharcnet.ca) for computing resources.

References and Notes

(1) Mouritsen, O. G. *Life—as a Matter of Fat. The Emerging Science of Lipidomics*; Springer Verlag: Heidelberg, Germany, 2005.
(2) Langer, R. *Nature (supp.)* **1998**, *392*, 5–10.
(3) Podgornik, R.; Harries, D.; DeRouchey, J.; Strey, H. H.; Parsegian, V. A. Interactions in macromolecular complexes used as non-viral vectors for gene delivery. In *Gene and Cell Therapy: Therapeutic Mechanisms and Strategies*, 3rd ed.; Templeton, N. S., Ed.; CRC: 2008; Chapter 7.
(4) Cevc, G. *Biochim. Biophys. Acta* **1990**, *1031*, 311–382.
(5) Israelachvili, J. *Intermolecular & surface forces*, 2nd ed.; Academic Press: San Diego, CA, 1991.
(6) Andelman, D. Introduction to electrostatics in soft and biological matter. *Proceedings of the Nato ASI & SUSSP on "Soft condensed matter physics in molecular and cell biology"*, New York, 2006; pp 97−122.
(7) Pashley, R. M. *J. Colloid Interface Sci.* **1981**, *80*, 153–162.
(8) Pashley, R. M.; Israelachvili, J. N. *J. Colloid Interface Sci.* **1984**, *101*, 511–523.
(9) Luo, G.; Malkova, S.; Yoon, J.; Schultz, D. G.; Lin, B.; Meron, M.; Benjamin, I.; Vanysek, P.; Schlossman, M. L. *Science* **2006**, *311*, 216–218.
(10) Marra, J. *Biophys. J.* **1986**, *50*, 815–825.
(11) Kekicheff, P.; Marcelja, S.; Senden, T. J.; Shubin, V. E. *J. Chem. Phys.* **1993**, *99*, 6098–6113.
(12) Fielden, M. L.; Hayes, R. A.; Ralston, J. *Phys. Chem. Chem. Phys.* **2000**, *2*, 2623–2628.
(13) Quesada-Perez, M.; Gonzalez-Tovar, E.; Martin-Molina, A.; Lozada-Cassou, M.; Hidalgo-Alvarez, R. *Colloids Surf., A* **2005**, *267*, 24–30.
(14) Angelini, T. E.; Golestanian, R.; Coridan, R. H.; Butler, J. C.; Beraud, A.; Krisch, M.; Sinn, H.; Schweizer, K. S.; Wong, G. C. L. *Proc. Natl. Acad. Sci.* **2006**, *103*, 7962–7967.
(15) *Electrostatic Effects in Soft Matter and Biophysics*; Holm, C., Kékicheff, P., Podgornik, R., Eds.; Kluwer Academic Publishers: Dordrecht, The Netherlands, 2001.
(16) Burak, Y.; Andelman, D. *Phys. Rev. E* **2000**, *62*, 5296–5312.
(17) Grosberg, A. Y.; Nguyen, T. T.; Shklovskii, B. I. *Rev. Mod. Phys.* **2002**, *74*, 329–345.
(18) Netz, R. R. *Eur. Phys. J. E* **2001**, *5*, 557–574.
(19) Patra, M.; Patriarca, M.; Karttunen, M. *Phys. Rev. E* **2003**, *67*, 031402.
(20) Punkkinen, O.; Naji, A.; Podgornik, R.; Vattulainen, I.; Hansen, P.-L. *Europhys. Lett.* **2008**, *82*, 48001.
(21) Falck, E.; Rog, T.; Karttunen, M.; Vattulainen, I. *J. Am. Chem. Soc.* **2008**, *130*, 44–45.
(22) McLaughlin, S. *Ann. Rev. Biophys. Chem.* **1989**, *18*, 113–136.
(23) Roux, M.; Bloom, M. *Biochemistry* **1990**, *29*, 7077–7089.
(24) Richardsen, H.; Vierl, U.; Cevc, G.; Fenzl, W. *Europhys. Lett.* **1996**, *34*, 543–548.
(25) Shoemaker, S. D.; Vanderlick, T. K. *Biophys. J.* **2002**, *83*, 2007–2014.
(26) Macdonald, P. M.; Seelig, J. *Biochemistry* **1988**, *27*, 6769–6775.
(27) Scherer, P. G.; Seelig, J. *Biochemistry* **1989**, *28*, 7720–7728.
(28) Hauser, H.; Phillips, M. C.; Levine, B. A.; Williams, R. J. P. *Nature* **1976**, *261*, 390–394.
(29) Lis, L. J.; Lis, W. T.; Parsegian, V. A.; Rand, R. P. *Biochemistry* **1981**, *20*, 1771–17777.
(30) Tatulian, S. A. *Eur. J. Biochem.* **1987**, *170*, 413–420.
(31) Clarke, R. J.; Lüpfert, C. *Biophys. J.* **1999**, *76*, 2614–2624.
(32) Binder, H.; Zschornig, O. *Chem. Phys. Lipids* **2002**, *115*, 39–61.
(33) Böckmann, R. A.; Hac, A.; Heimburg, T.; Grubmüller, H. *Biophys. J.* **2003**, *85*, 1647–1655.
(34) Petrache, H. I.; Kimchi, I.; Harries, D.; Parsegian, V. A. *J. Am. Chem. Soc.* **2005**, *127*, 11546–11547.
(35) Garcia-Manyes, S.; Oncins, G.; Sanz, F. *Biophys. J.* **2005**, *89*, 1812–1826.

(36) Garcia-Manyes, S.; Oncins, G.; Sanz, F. *Electrochim. Acta* **2006**, *51*, 5029–5036.
(37) Petrache, H. I.; Tristram-Nagle, S.; Harries, D.; Kucerka, N.; Nagle, J. F.; Parsegian, V. A. *J. Lipid Res.* **2006**, *47*, 302–309.
(38) Petrache, H. I.; Zemb, T.; Belloni, L.; Parsegian, V. A. *Proc. Natl. Acad. Sci.* **2006**, *103*, 7982–7987.
(39) Aroti, A.; Leontidis, E.; Dubois, M.; Zemb, T. *Biophys. J.* **2007**, *93*, 1580–1590.
(40) Fukuma, T.; Higgins, M. J.; Jarvis, S. P. *Phys. Rev. Lett.* **2007**, *98*, 106101.
(41) Pabst, G.; Hodzic, A.; Strancar, J.; Danner, S.; Rappolt, M.; Laggner, P. *Biophys. J.* **2007**, *93*, 2688–2696.
(42) Pandit, S. A.; Bostick, D.; Berkowitz, M. L. *Biophys. J.* **2003**, *84*, 3743–3750.
(43) Sachs, J. N.; Woolf, T. B. *J. Am. Chem. Soc.* **2003**, *125*, 8742–8743.
(44) Böckmann, R. A.; Grubmüller, H. *Angew. Chem., Int. Ed.* **2004**, *43*, 1021–1024.
(45) Sachs, J. N.; Nanda, H.; Petrache, H. I.; Woolf, T. B. *Biophys. J.* **2004**, *86*, 3772–3782.
(46) Gurtovenko, A. A. *J. Chem. Phys.* **2005**, *122*, 244902.
(47) Gurtovenko, A. A.; Vattulainen, I. *J. Am. Chem. Soc.* **2005**, *127*, 17570–17571.
(48) Tepper, H. L.; Voth, G. A. *J. Phys. Chem. B* **2006**, *110*, 21327–21337.
(49) Shinoda, K.; Shinoda, W.; Mikami, M. *Phys. Chem. Chem. Phys.* **2007**, *9*, 643–650.
(50) Gurtovenko, A. A.; Vattulainen, I. *Biophys. J.* **2007**, *92*, 1878–1890.
(51) Lee, S.-J.; Song, Y.; Baker, N. A. *Biophys. J.* **2008**, *94*, 3565–3576.
(52) Gurtovenko, A. A.; Vattulainen, I. *J. Phys. Chem. B* **2008**, *112*, 1953–1962.
(53) Cordomi, A.; Edholm, O.; Perez, J. J. *J. Phys. Chem. B* **2008**, *112*, 1397–1408.
(54) Pandit, S. A.; Berkowitz, M. L. *Biophys. J.* **2002**, *82*, 1818–1827.
(55) Pandit, S. A.; Bostick, D.; Berkowitz, M. L. *Biophys. J.* **2003**, *85*, 3120–3131.
(56) Mukhopadhyay, P.; Monticelli, L.; Tieleman, D. P. *Biophys. J.* **2004**, *86*, 1601–1609.
(57) Pedersen, U. R.; Leidy, C.; Westh, P.; Peters, G. H. *Biochim. Biophys. Acta* **2006**, *1758*, 573–582.
(58) Zhao, W.; Rog, T.; Gurtovenko, A. A.; Vattulainen, I.; Karttunen, M. *Biophys. J.* **2007**, *92*, 1114–1124.
(59) Faraudo, J.; Travesset, A. *Biophys. J.* **2007**, *92*, 2806–2818.
(60) Gurtovenko, A. A.; Patra, M.; Karttunen, M.; Vattulainen, I. *Biophys. J.* **2004**, *86*, 3461–3472.
(61) Gurtovenko, A. A.; Miettinen, M.; Karttunen, M.; Vattulainen, I. *J. Phys. Chem. B* **2005**, *109*, 21126–21134.
(62) Patra, M.; Karttunen, M. *J. Phys. Chem. B*, submitted for publication, **2007**.
(63) Rigaud, J. L.; Gary-Bobo, C. M. *Biochim. Biophys. Acta* **1977**, *469*, 246–256.
(64) Huxley, A. F.; Stampeli, R. *J. Physiol.* **1949**, *108*, 315–339.
(65) Hodgkin, A. L.; Huxley, A. F. *J. Physiol.* **1952**, *116*, 449–472.
(66) Mulkidjanian, A. Y.; Dibrov, P.; Galperin, M. Y. *Biochim. Biophys. Acta* **2008**, *1777*, 985–992.
(67) Antonenko, Y. N.; Pohl, P. *FEBS Lett.* **1998**, *429*, 197–200.
(68) Alexiev, U.; Mollaaghababa, R.; Scherrer, P.; Khorana, H.; Heyn, M. *Proc. Natl. Acad. Sci.* **1995**, *92*, 372–376.
(69) Heberle, J.; Riesle, J.; Thiedemann, G.; Oesterhelt, D.; Dencher, N. A. *Nature* **1994**, *370*, 379–382.
(70) Berger, O.; Edholm, O.; Jahnig, F. *Biophys. J.* **1997**, *72*, 2002–2013.
(71) http://www.softsimu.org/downloads.shtml.
(72) Berendsen, H. J. C.; van der Spoel, D.; van Drunen, R. *Comput. Phys. Commun.* **1995**, *91*, 43–56.
(73) Lindahl, E.; Hess, B.; van der Spoel, D. *J. Mol. Model.* **2001**, *7*, 306–317.
(74) van der Spoel, D.; Lindahl, E.; Hess, B.; Groenhof, G.; Mark, A. E.; Berendsen, H. J. C. *J. Comput. Chem.* **2005**, *26*, 1701–1718.
(75) Berendsen, H. J. C.; Postma, J. P. M.; van Gunsteren, W. F.; Hermans, J. Interaction models for water in relation to protein hydration. In *Intermolecular Forces*; Pullman, B., Ed.; Reidel: Dordrecht, The Netherlands, 1981; pp 331−342.
(76) Darden, T.; York, D.; Pedersen, L. *J. Chem. Phys.* **1993**, *98*, 10089–10092.
(77) Essman, U.; Perela, L.; Berkowitz, M. L.; T.; Darden, H. L.; Pedersen, L. G. *J. Chem. Phys.* **1995**, *103*, 8577–8592.
(78) Patra, M.; Karttunen, M.; Hyvönen, M. T.; Lindqvist, P.; Falck, E.; Vattulainen, I. *Biophys. J.* **2003**, *84*, 3636–3645.
(79) Anézo, C.; de Vries, A. H.; Höltje, H.-D.; Tieleman, D. P.; Marrink, S.-J. *J. Phys. Chem. B* **2003**, *107*, 9424–9433.
(80) Patra, M.; Karttunen, M.; Hyvönen, M. T.; Falck, E.; Vattulainen, I. *J. Phys. Chem. B* **2004**, *108*, 4485–4494.
(81) Hess, B.; Bekker, H.; Berendsen, H. J. C.; Fraaije, J. G. E. M. *J. Comput. Chem.* **1997**, *18*, 1463–1472.
(82) Miyamoto, S.; Kollman, P. A. *J. Comput. Chem.* **1992**, *13*, 952–962.
(83) Enders, O.; Ngezahayo, A.; Wiechmann, M.; Leisten, F.; Kolb, H.-A. *Biophys. J.* **2004**, *87*, 2522–2531.
(84) Lewis, R. N. A. H.; Tristram-Nagle, S.; Nagle, J. F.; McElhaney, R. N. *Biochim. Biophys. Acta* **2001**, *1510*, 70–82.
(85) Zantl, R.; Baicu, L.; Artzner, F.; Sprenger, I.; Rapp, G.; Rädler, J. O. *J. Phys. Chem. B* **1999**, *103*, 10300–10310.
(86) Berendsen, H. J. C.; Postma, J. P. M.; van Gunsteren, W. F.; DiNola, A.; Haak, J. R. *J. Chem. Phys.* **1984**, *81*, 3684–3690.
(87) Filippov, A.; Orädd, G.; Lindblom, G. *Biophys. J.* **2003**, *84*, 3079–3086.
(88) Gennis, R. B. *Biomembranes. Molecular Structure and Function*; Springer Advanced Texts in Chemistry; Springer: New York, 1989.
(89) Flenner, E.; Das, J.; Rheinstadter, M. C.; Kosztin, I. *Phys. Rev. E* **2009**, *79*, 011907.
(90) Murzyn, K.; Zhao, W.; Karttunen, M.; Kurdziel, M.; Róg, T. *Biointerphases* **2006**, *1*, 98–105.
(91) Boström, M.; Lima, E. R. A.; Tavares, F. W.; Ninham, B. W. *J. Chem. Phys.* **2008**, *128*, 135104.
(92) Zhang, L.; Spurlin, T. A.; Gewirth, A. A.; Granick, S. *J. Phys. Chem. B* **2006**, *110*, 33–35.
(93) Brändén, M.; Sandén, T.; Brzezinski, P.; Widengren, J. *Proc. Natl. Acad. Sci.* **2006**, *103*, 19766–19770.
(94) Collins, K. *Proc. Natl. Acad. Sci.* **1995**, *92*, 5553–5557.
(95) Collins, K. D. *Biophys. J.* **1997**, *72*, 65–76.
(96) Tieleman, D. P.; Berendsen, H. J. C. *J. Chem. Phys.* **1996**, *105*, 4871–4880.
(97) Lindahl, E.; Edholm, O. *Biophys. J.* **2000**, *79*, 426–433.
(98) Patra, M.; Karttunen, M. *J. Comput. Chem.* **2004**, *25*, 678–689.
(99) Auffinger, P.; Cheatham, T. E.; Vaiana, A. C. *J. Chem. Theory Comput.* **2007**, *3*, 1851–1859.

JP810233Q